2005 International Symposium on Nonlinear
Theory and its Applications (NOLTA2005)
Bruges, Belgium, October 18-21, 2005

A study on vibration characteristics of microcantilever probe near period-doubling bifurcation

Kohei YAMASUE † and Takashi HIKIHARA†

†Department of Electrical Engineering, Kyoto University
Katsura, Nishikyo, Kyoto 615-8510, Japan
Email: yamasue@dove.kuee.kyoto-u.ac.jp

Abstract—A numerical study on force sensitivity of dynamic force microscopy is carried out near period-doubling bifurcation of microcantilever vibration. A small periodic signal is additionally given to the driving signal of the microcantilever to utilize sensitive dependence of vibration on tip-sample distance. The additional periodic signal proposed here readily achieves the same effects as parametric excitation which has been employed for enhancing sensitivity.

1. Introduction

In 1986, G. Binnig, C. F. Quate and Ch. Gerber have introduced the atomic force microscopy [1]. Among its operation modes, the dynamic force microscopy (DFM) has made remarkable progress toward a core technology for nanoscience and nanoengineering [2, 3]. The DFM allows us to investigate material surfaces in nanometer resolution without damaging samples [4]. There are also many applications of the DFM including measurement of various surface properties [5, 6, 7], manipulation of single atoms [8], and control of surfaces [9].

A key device of the DFM is a vibrating microcantilever sensor to detect the tiny interaction force between a sharp tip manufactured at the free end of the microcantilever and sample surface confronting the tip. The vibrating microcantilever shows a variety of nonlinear phenomena especially when it is placed in close proximity of the surface. The microcantilever vibrating in nonlinear tip-sample interaction force exhibits period-doubling bifurcation [10, 11] and bistability involving jumping and hysteresis [12, 13, 14, 15, 16]. In addition, Ashhab *et. al* and Basso *et al.* have predicted chaotic vibration near surfaces theoretically [17, 18] and numerically [19]. An experimental study by Jamitzky *et. al* has recently clarified period-doubling route to chaos actually occurs in close proximity of a sample surface [20].

These significant works have motivated researchers to develop measurement techniques using nonlinear dynamics of vibrating microcantilevers [21]. In particular, Patil *et al.* have proposed enhancing force sensitivity by parametric excitation of a microcantilever near period-doubling bifurcation [11]. This strategy is based on the idea that dynamical systems near period-doubling bifurcation can be utilized as a small signal amplifier [22, 23]. The parametric excitation modulating the tip-sample distance was experimentally performed by shaking the sample vertically or scanning periodic lattice structures of single crystals. However, it is preferable to avoid shaking sample by the scanner of DFM. The scanners are primarily designed to position samples spatially and therefore difficult to drive at high frequency.

In this paper, we propose applying a small periodic signal to the driving force of the microcantilever. The frequency of the applied signal is a half of driving frequency and its amplitude is much smaller than the driving amplitude. The applied small periodic signal and the parametric excitation are shown to have the same effects on vibration characteristics for tip-sample distance. The proposed technique is easy to apply in the actual DFM systems without shaking scanners.

2. Mathematical model of microcantilever probe near sample surfaces

A schematic diagram of the dynamic force microscopy is shown in Fig. 1. The microcantilever is excited at or near its mechanical resonant frequency during measurement. When the tip of microcantilever is placed close to a sample surface, the resonance frequency is varied depending on the tip-sample interaction force governed by their distance. The shift of the resonant frequency is measured by amplitude modulation [4] or frequency modulation [24]. The topography of sample is acquired by raster-scanning of the surface with keeping the vibration constant. The vibration is typically measured by the optical lever method [25].

The first mode vibration of microcantilever is described by the following differential equation, when the tip-sample interaction force is approximated by Lennard-Jones potential function [17]:

$$\begin{cases} \dot{\xi}_1 = \xi_2 \\ \dot{\xi}_2 = -\xi_1 - \dfrac{d}{(\alpha(t)+\xi_1)^2} + \dfrac{\Sigma^6 d}{30(\alpha(t)+\xi_1)^8} \\ \qquad +\varepsilon(\Gamma\cos\Omega t - \Delta\xi_2) + p(t), \end{cases} \tag{1}$$

where $\alpha(t)$ denotes the equilibrium point of the tip, when only the gravity acts on it. (ξ_1, ξ_2) is the dis-

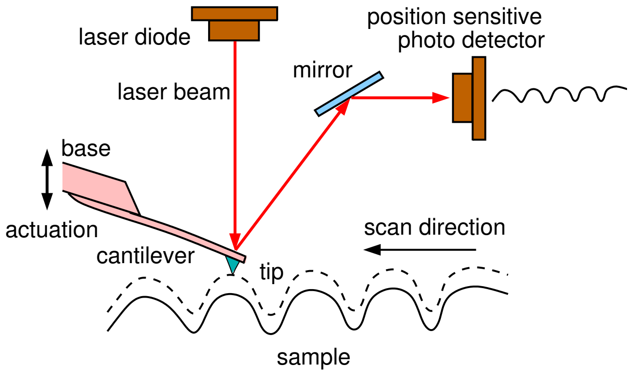

Figure 1: Operation of dynamic force microscopy. Sample surface is scanned by microcantilever probe vibrating at its resonant frequency. The mean distance between the apex of tip and the surface of sample is maintained constant by scanner device which control the height of the sample surface. The vibration of cantilever is typically measured by optical lever method.

placement and velocity of the tip. $p(t)$ is the perturbation input to microcantilever. (Ω, Γ) denotes the freqency and amplitude of the sinusoidal external force driving microcantilever. Σ is diameter of molecular composing sample and tip. $d = 4/27$ is a constant. ε is a small parameter. It should be noted that Eq. (1) is dimensionless. It has been shown that the motion of microcantilever can be chaotic by applying the Melnikov method to Eq. (1) under $\alpha(t) = \alpha_0$ constant and $p(t) = 0$ [17, 18].

Hereafter, we consider the following three cases. The first is denoted by case 1 that parametric excitation nor additional periodic signal are not applied. The condition is described as follows:

$$\begin{cases} \alpha(t) = \alpha_0 \\ p(t) = 0. \end{cases} \tag{2}$$

The DFM is typically operated under this condition.

The second is case 2 where the microcantilever is parametrically excited by modulating tip-sample distance at the frequency $\omega = \Omega/2$. In this case, the $\alpha(t)$ is written as follows:

$$\begin{cases} \alpha(t) = \alpha_0 + \varepsilon\gamma\cos\omega t \\ p(t) = 0, \end{cases} \tag{3}$$

where γ is the amplitude of parametric excitation satisfying $\gamma \ll \Gamma$.

case 3 is the case in which a small periodic signal is additionally given to the driving force of the microcantilever:

$$\begin{cases} \alpha(t) = \alpha_0 \\ p(t) = \varepsilon\gamma\cos\omega t, \end{cases} \tag{4}$$

where γ and ω denote the amplitude and frequency of the periodic signal satisfying $\gamma \ll \Gamma$ and $\omega = \Omega/2$, respectively. The symbols are the same as in case 3 for simplicity of notation.

3. Effects of small periodic signal given to microcantilever drive

Patil *et. al* have experimentally discussed the possibility of enhancing force sensitivity by exciting the scanner at a few Hertz much smaller than the driving frequency 11.2 kHz [11]. However, perturbing scanners is not preferable, because the scanners have to adjust the height of sample in subnanometer resolution during measurement. In this paper, a small perodic signal is superimposed to driving signal as an alternative for the parametric excitation.

To begin with, we should show that the superimposed signal has the same effect as the parametric excitation. In the parametric excitation (case 2) described by Eq. (3), the attractive and repulsive interactions are approximated as follows:

$$\begin{aligned} -\frac{d}{(\alpha+\xi_1)^2} &= -d\Big[\frac{1}{(\alpha_0+\xi_1)^2} - \frac{2}{(\alpha_0+\xi_1)^3}\varepsilon\gamma\cos\omega t \\ &\qquad + \frac{3}{(\alpha_0+\xi_1)^4}\varepsilon^2\gamma^2\cos^2\omega t - \cdots\Big] \\ &\approx -d\Big[\frac{1}{(\alpha_0+\xi_1)^2} - \frac{2}{(\alpha_0+\xi_1)^3}\varepsilon\gamma\cos\omega t\Big], \end{aligned} \tag{5}$$

$$\begin{aligned} \frac{\Sigma^6 d}{30(\alpha+\xi_1)^8} &= \frac{\Sigma^6 d}{30}\Big[\frac{1}{(\alpha_0+\xi_1)^8} - \frac{8}{(\alpha_0+\xi_1)^9}\varepsilon\gamma\cos\omega t \\ &\qquad + \frac{36}{(\alpha_0+\xi_1)^{10}}\varepsilon^2\gamma^2\cos^2\omega t - \cdots\Big] \\ &\approx \frac{\Sigma^6 d}{30}\Big[\frac{1}{(\alpha_0+\xi_1)^8} - \frac{8}{(\alpha_0+\xi_1)^9}\varepsilon\gamma\cos\omega t\Big]. \end{aligned} \tag{6}$$

The approximation is valid, assuming that γ is small enough to satisfy the relation $|\varepsilon\gamma| \ll |\alpha_0 + \xi_1|$. Although the assumption may fail when the tip comes to collide against the surface, it occurs instantaneously and therefore the influence is negligible to discuss the effects of the parametric excitation. Substituting Eqs. (5) and (6) to Eq. (1), the following equation is derived:

$$\begin{cases} \dot{\xi_1} = \xi_2 \\ \dot{\xi_2} = -\xi_1 - \dfrac{d}{(\alpha_0+\xi_1)^2} + \dfrac{\Sigma^6 d}{30(\alpha_0+\xi_1)^8} \\ \qquad +\varepsilon(\Gamma\cos\Omega t - \Delta\xi_2) + p(t), \end{cases} \tag{7}$$

where $p(t)$ is given by

$$p(t;\alpha_0) = \Big[\frac{2d}{(\alpha_0+\xi_1)^3} - \frac{8\Sigma^6 d}{30(\alpha_0+\xi_1)^9}\Big]\varepsilon\gamma\cos\omega t. \tag{8}$$

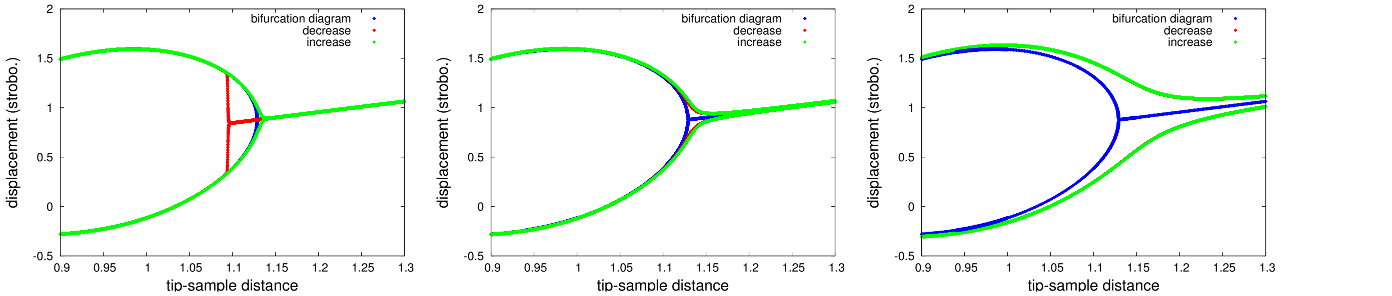

(a) Normal operation (case 1) (b) With parametric excitation (case 2) (c) With small periodic signal (case 3)

Figure 2: Bifurcation diagram and characteristic curves of displacement of microcantilever on tip-sample distance near period-doubling bifurcation point. The characteristics curves show stroboscopic plots of displacement for monotonously increasing and decreasing tip-sample distance. Frequency of stroboscopic plots equals to the driving frequency. The change of vibration is much delayed by long transient near the bifurcation point.

It is shown that $p(t)$ has a component whose frequency equals to a half of the driving frequency, by taking the fundamental component with respect to the terms enclosed in the brackets:

$$p(t;\alpha_0) \tag{9}$$

$$= \{2C(\alpha_0)\cos(\Omega t - \theta(\alpha_0))\}\,\varepsilon\gamma\cos\omega t + (\text{other components})$$

$$= C(\alpha_0)\varepsilon\gamma\cos\left(\frac{\Omega}{2}t - \theta(\alpha_0)\right) + (\text{other components}), \tag{10}$$

where $C(\alpha_0)$ and $\theta(\alpha_0)$ is a Fourier coefficient and phase difference depending on α_0. If we assume α_0 is constant under steady states, Eq.(4) is derived by neglecting the phase difference and rewriting $C(\alpha_0)\varepsilon\gamma$ as $\varepsilon\gamma$. Thus, it is reasonable that the parametric excitation and small periodic signal have the same effects under steady states, while there is a difference that the amplitude of $p(t)$ is not varied depending on the tip-sample distance in the case of small periodic signal. However, we will show the difference does not play a role in enhancement of the force sensitivity using the period doubling bifurcation.

4. Vibration characteristics near period-doubling bifurcation

We here numerically compare the vibration characteristics in the three cases described by Sec. 2 near the period-doubling bifurcation point. The characteristic curves of displacement of microcantilever on tip-sample distance are shown in Figs. 2(a), 2(b), 2(c). These characteristic curves show the stroboscopic plots of displacement obtained by monotonously increasing and decreasing the tip-sample distance. The frequency of plots equals to the driving frequency. Note that the curves are influenced by the transient states of vibration because of nonzero sweep rate. The bifurcation diagrams constructed by the Newton-Raphson method are also shown in these figures to depict the influence of transient states. The parameters are here configured at $(\Sigma,\ \Gamma,\ \varepsilon,\ \Omega,\ \Delta,\ \gamma) = (0.3,\ 10,\ 0.1,\ 1.0,\ 0.4,\ 0.01)$.

case 1 (Fig. 2(a))

When the tip-sample distance is reduced, the vibration of microcantilever meets a bifurcation point at which the period of the vibration is doubled. Before the bifurcation occurs, the frequency is the same to that of the excitation and variation of the displacement for tip-sample distance is small. On the other hand, the displacement is drastically changed immediately after the period-doubling bifurcation and therefore the force sensitivity can be increased. However, the two curves show transient characteristics that is not suitable for surface measurement. The curves do not follow the bifurcation diagram near the bifurcation point. The change of vibration is delayed due to long transient not bistability.

case 2 (Fig. 2(b))

In the whole range, the period of vibration is 4π due to the parametric excitation at the frequency $\Omega/2$. The displacement is rapidly changed around the original bifurcation point, while the force sensitivity seems to be relaxed compared to case 1. The transient is also much reduced. The curves coincide to those as in case 1, where the tip-sample distance is far from the bifurcation point.

case 3 (Fig. 2(c))

The period of vibration is 4π due to the additional small periodic signal with frequency $\Omega/2$. As in case 2, the relaxed change of displacement is observed near the original bifurcation point and the long transient is also suppressed. In addition, the vibration far from the bifurcation point is not largely changed by the additional small perturbation.

We here notice that the parametric excitation (case 2) and the small periodic signal (case 3) have qualitatively same effects on the vibration characteristics. Both techniques suppress the long transient state near the bifurcation point. The case 3 seems better than case 2, because the parametric excitation by shaking scanner is not preferable from the point of the primary roles of the scanner. The hysteresis characteristics of piezo scanners disturbs precise control of the height of sample surface. Figure 3 shows the dependence of displacement on the amplitude of the additional periodic signal at the bifurcation point. The continuous dependence on the amplitude implies that the force sensitivity can be adjusted by varying the amplitude of periodic signal.

5. Conclusion

In this paper, we have numerically discussed the force sensitivity of the DFM near the period-doubling bifurcation. The additional small periodic signal to microcantilever drive improves the vibration characteristics near the bifurcation point. The proposed technique is easily applied to actual DFM systems and also has the same effects as the parametric excitation that can enhance the force sensitivity of DFM. The subharmonic component is available for measurement because of its rapid increase near period-doubling bifurcation point.

Acknowledgments

This work was partly supported by the Japan Society for the Promotion of Science (JSPS) the 21st Century COE Program (Grant No. 14213201).

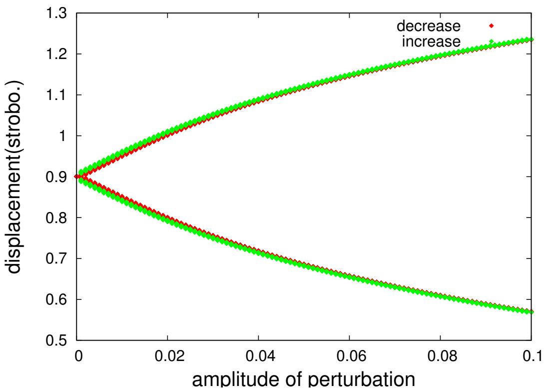

Figure 3: Dependence of displacement of cantilever on amplitude of additional small signal

References

[1] G. Binning, C. F. Quate, and Ch. Gerber, Phys. Rev. Lett., **56**, 930–933 (1986).

[2] F. J. Giessibl, Rev. Mod. Phys., **75**, 949–983 (2003).

[3] R. García and R. Pérez, Surf. Sci. Rep., **47**, 197–301 (2002).

[4] Y. Martin, C. C. Williams, and H. K. Wickramasinghe, J. Appl. Phys., **61** (4), 4723–4729 (1987).

[5] Y. Martin and H. K. Wickramasinghe, Appl. Phys. Lett., **50** (20), 1455–1457 (1987).

[6] J. E. Stern, B. D. Terris, H. Mamin, and D. Rugar, Appl. Phys. Lett., **53** (26), 2717–2719 (1988).

[7] M. Nonnenmacher, M. P. O'Boyle, and H. K. Wickramasinghe, Appl. Phys. Lett., **58** (25), 2921–2923 (1991).

[8] Y. Sugawara, Y. Sano, N. Suehira, and S. Morita, Applied Surface Science, **188** (3-4), 285–291 (2002).

[9] N. Sasaki, S. Watanabe, and M. Tsukada, Phys. Rev. Lett., **88** (4), 046101 (2002).

[10] N. A. Burnham, A. J. Kulik, G. Germaud, and G. A. D. Briggs, Phys. Rev. Lett., **74**, 5092–5095 (1995).

[11] S. Patil and C. V. Dharmadhikari, Appl. Surf. Sci, **217**, 7–15 (2003).

[12] P. Gleyzes, P. K. Kuo, and A. C. Boccara, Appl. Phys. Lett., **58** (25), 2989–2991 (1991).

[13] N. Sasaki, M. Tsukada, R. Tamura, K. Abe, and N. Sato, Appl. Phys. A, **66**, S287–S291 (1998).

[14] J. P. Aimé, R. Boisgard, L. Nony, and G. Couturier, Phys. Rev. Lett., **82** (17), 3388–3391 (1999).

[15] R. García and A. S. Paulo, Phys. Rev. B, **61** (20), R13381–R13384 (2000).

[16] S. Rutzel, S. I. Lee, and A. Raman, Proc. R. Soc. Lond. A, **459** (2036), 1925–1948 (2003).

[17] M. Ashhab, M. V. Salapaka, M. Dahleh, and I. Mezić, Nonlin. Dynam, **20**, 197–220 (1999).

[18] M. Ashhab, M. V. Salapaka, M. Dahleh, and I. Mezić, Automatica, **35**, 1663–1670 (1999).

[19] M. Basso, L. Giarre, M. Dahleh, and Mezić, J. Dynam. Syst. Meas. Control, **122**, 240–245 (2000).

[20] F. Jamitzky, M. Stark, W. Bunk, W. M. Heckl, and R. W. Stark, Proc. 2004 4th IEEE Conf. Nanotechnology, 38–40 (2004).

[21] R. W. Stark and W. M. Heckl, Rev. Sci. Instrum., **74** (12), 5111–5114 (2003).

[22] K. Wiesenfeld and B. McNamara, Phys. Rev. Lett., **55** (1), 13–16 (1985).

[23] K. Wiesenfeld and B. McNamara, Phys. Rev. A, **33** (1), 629–642 (1986).

[24] T. R. Albrecht, P. Grutter, D. Horne, and D. Rugar, J. Appl. Phys., **69**, 668–673 (1991).

[25] G. Meyer and M. Amer, Appl. Phys. Lett., **53**, 1045–1047 (1988).